Michał KRUK[1], Bartosz ŚWIDERSKI[1], Stanisław OSOWSKI[2,3]

University of Life Sciences (1), Warsaw University of Technology (2), Military University of Technology (3),

Box-counting fractal dimension in application to recognition of hypertension through the retinal image analysis

Abstract. *The paper presents the application of the box-counting dimension to the recognition of hypertension through the analysis of the image of the eye fundus. The box-counting dimension represents a single measure, often used to describe the structure of fractal-like images. We propose based on it fast method of classification of the retinal image in order to recognize the class of healthy, introductory step and advanced illness cases. The results of experiments performed on 125 cases confirm good performance of the proposed method.*

Streszczenie. *Praca prezentuje zastosowanie wymiaru pudełkowego do rozpoznania zmian ciśnieniowych poprzez automatyczna analizę obrazu dna oka. Zaproponowana została metoda szybkiego rozpoznania stanu chorobowego rozróżniająca trzy klasy: zdrowi, początkowy stan choroby i stan zaawansowany. Przedstawione są rezultaty rozpoznania dotyczące 125 przypadków. (**Zastosowanie wymiaru pudełkowego do rozpoznania zmian ciśnieniowych poprzez automatyczna analizę obrazu dna oka**)*

Keywords: retinal image processing, box-counting fractal dimension, image segmentation and classification
Słowa kluczowe: obraz dna oka, fraktale, wymiar pudełkowy, segmentacja i rozpoznawanie obrazu

Introduction

Examination of the eye fundus images plays an important role in diagnosis of arterial hypertension and diabetes. Several changes are observed when illness start or is in an advanced stage. The detailed description of the degree of development of the illness, uses five-point scale [1]. The association of this scale with the view of the fundus of the eye is presented in Fig 1. The succeeding images represent typical vessel structures of eye fundus at different stages of the development of the artery hypertension.

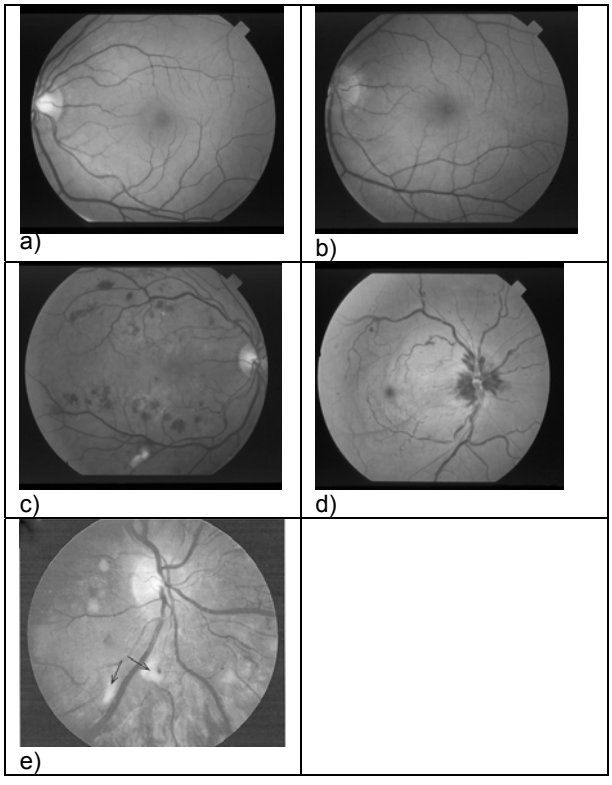

Fig.1. The typical images of the eye fundus at different stages of the development of the illness. a) Healthy stage, b) Stage 1 (angiopathia hypertonica retinae) c) Stage 2 (angiosclerosis hypertonica retinae) d) Stage 3 (retinopathia hyperthonica maligna), e) Stage 4 (neurorethinopathia hyperthonica retinae maligna)

Fig. 1a corresponds to the healthy stage, and the other images (b,c,d,e) to succeeding stages of the illness. In practice we usually recognize only three classes: healthy case (class 1), the first two stages of illness (class 2) and the last advanced stages (class 3). Looking at the network of the blood vessels in the eye we can associate it with the fractals. Hence it is natural to apply the fractal measures to characterize the vessel structure of the eye fundus.

The paper is concerned with the characterization of the images of eye fundus using the box-counting dimension, the measure of similarity, taken form fractal theory. Short description of this way of characterization of fractal structure will be first introduced. Next we will show, that application of this measure is useful for recognizing the healthy case from the others, representing different stages of the artery hypertension illness.

In further analysis we will consider three classes of images. Each of the class is characterized by different structure of the blood vessels, resembling the fractals. Application of box-counting dimension will allow to find the reliable numerical descriptor characterizing the changes of the eye fundus.

Application of the box-counting dimension in recognition of retina is not quite new. It has been already applied [2] in biometrics for authentication of different individuals. Our work is directed to show its applicability to recognize different stages of arterial hypertension on the basis of the image of eye fundus.

Box-counting fractal dimension

Fractals are typically self-similar patterns, which means that after fragmentation of the geometric shape each of the subdivided region is approximately a reduced copy of the whole [3]. The fractal dataset has roughly the same statistical properties for a wide variation in scale or size. There are many different measures applicable to fractals, such as fractional Brownian motion, Hausdorff-Besicovitch dimension and many others [3], but they are calculated in complicated way and the computational cost is usually high.

The box-counting fractal dimension is a very simple measure characterizing the fractal complexity. It is the particular case of the Mandelbrot fractal dimension and is based on the notion of self-similarity of the structure at different scales. In principle it measures how the length of the complex curve is changing when the measurement is performed with the increased accuracy [3].

Let us assume that the object under characterization, for example curve, is placed on the surface covered with the set of regular cubes (squares in 2-dimensional space or hexahedron in 3-dimensional space) of the size ε. We count the number of cubes that contain any fragment of the curve. This number is evidently dependent on the size of ε. Let us denote it as N(ε). Changing the size ε we get different values of N(ε), generally increasing when ε is decreased. Next we define the relation

(1) $$\log\big(N(\varepsilon)\big) = f\big(\log(1/\varepsilon)\big)$$

and calculate its slope *d*, defined as

(2) $$d = -\lim_{\varepsilon \to 0} \frac{\log\big(N(\varepsilon)\big)}{\log(\varepsilon)}$$

In practice instead of ε we use the number s^2 of elementary cubes, each of the size ε, fixed on the considered analyzed squared area. The value of s is inversely proportional to ε. So the last equation might be rewritten in the form

(3) $$d = \lim_{s \to \infty} \frac{\log\big(N(s)\big)}{\log(s)}$$

The value d represents the box-counting dimension, characterizing the complexity of the curve. To use the box-counting notion we have to define only one parameter – the number of boxes N(s), dependent on *s*. The number s defines the size of the binary matrix s×s. We check if any fragment of the curve enters each box. If yes, we put one in proper location of the matrix, in other case zero.

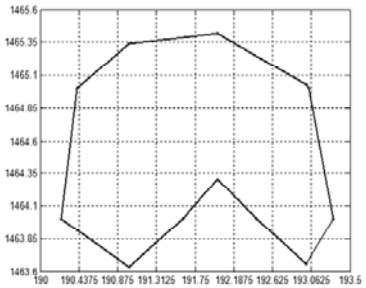

Fig.2 The illustrative example how to calculate N(s) for s=8

To illustrate the procedure we consider the curve (solid line) presented on the background of the square decomposed into 8×8 cubes (Fig. 2). In this case *s*=8 defines the binary matrix of the size 8×8. Simple inspection of the curve illustrated in Fig. 2 reveals that the binary matrix **M** illustrating appearance of curve in the respective boxes takes the form

$$\mathbf{M} = \begin{bmatrix} 0 & 0 & 1 & 1 & 1 & 0 & 0 & 0 \\ 0 & 1 & 1 & 0 & 1 & 1 & 1 & 0 \\ 1 & 1 & 0 & 0 & 0 & 0 & 1 & 1 \\ 1 & 0 & 0 & 0 & 0 & 0 & 0 & 1 \\ 1 & 0 & 0 & 0 & 0 & 0 & 0 & 1 \\ 1 & 0 & 0 & 1 & 1 & 1 & 0 & 1 \\ 1 & 1 & 0 & 1 & 0 & 1 & 1 & 1 \\ 0 & 1 & 1 & 1 & 0 & 0 & 1 & 1 \end{bmatrix}$$

Now the boxes containing fragments of the curve are represented in this matrix by ones. It is evident that their number is equal N(s) = 32. In general, at changing value of s the number N(s) is also changing. Table 1 presents the changes of N(s) as a function of s.

Table 1 The change of N(s) versus different values of s

s	4	8	16	32	64
N(s)	14	32	65	134	267

Fig. 3 presents the relationship between s and N(s) in logarithmic scale at different values of s corresponding to the values depicted in Table 1 (the solid blue line).

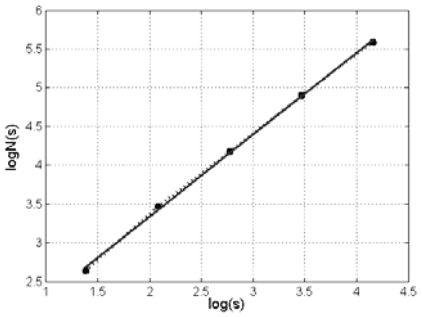

Fig.3. The relationship N(s) =f(s) in logarithmic scale (the dotted line) and its linear representation (the solid line)

To find the slope of this relationship in logarithmic scale we have to build the general linear regression expressed in the form:

(4) $$\log(N(s)) = \alpha + \beta \log(s) + \Delta$$

with Δ representing the error of a linear approximation. After performing the linear regression of the curve of Fig. 3 we have got the following form of linear equation

$$\log\big(N(s)\big) = 1.2215 + 1.0573 \log(s) + \Delta$$

The slope of this curve is equal to the box-counting dimension *d*=1.0573.

The procedure of determination of box-counting dimension may be easily applied for real grey scale images. However, in such case we have to apply first the edge detection algorithms, for example filtering the image by using proper mask (Canny, Previtt, Sobel, etc.) or by applying the morphological operations. In this way the image will be presented in a binary contour form, for which we can directly apply the estimation procedure of the box-counting dimension, presented above.

Application of box-counting dimension for retinal image recognition

In this section we will apply the concept of box-counting dimension to the classification of changes in retinal images. There are few steps leading to the final results of recognition:

- extraction of the vascular tree,
- evaluation of the box-counting dimension,
- classification of images based on the principle of distance between the box-counting measures.

Vascular Tree Extraction

The vascular tree is the most prominent anatomical structure in the retina and the results of its analysis play an important role in diagnosis of the hypertension estimation of the human [5,6,7]. The typical views of the eye fundus at different stages of the development of illness were given in Fig.1. The difficult point in further processing of these images is the accurate extraction of the structure of the small blood vessels. In this paper we have used the algorithm described in [5]. Its main stages may be summarized in following steps:

1. Enhancement of the prominent blood vessels using the 2-dimensional match filtering.
2. Application of local entropy based thresholding, well preserving the spatial structure in the binarized image [8].
3. Thinning of the vascular tree using the morphological operations [9].

The most important point of the algorithm is to determine of an optimal threshold value using the local-entropy

maximization. The first step is to apply the Haralick GLCM texture algorithm based on the co-occurrence matrix [10] by considering the horizontally right and vertically lower transitions. By denoting the probability of co-occurrence of gray levels i and j by p_{ij} and assuming $0 \le s \le L-1$, where L is the number of intensity levels, we define the quantities

(6) $$P_A = \sum_{i=0}^{s}\sum_{j=0}^{s} p_{ij}$$

(7) $$P_B = \sum_{i=s+1}^{L-1}\sum_{j=s+1}^{L-1} p_{ij}$$

On the basis of this we define two normalized probabilities of co-ocurrance of gray levels *i* and *j* as follows

(8) $$P_{ij}^{A} = \frac{p_{ij}}{P_A}$$

(9) $$P_{ij}^{B} = \frac{p_{ij}}{P_B}$$ Index

A in this expression denotes the object and B – the background. The total local entropy of the object and the background is defined in the form [8]

(10) $$H_T(s) = -\frac{1}{2}\left[\sum_{i=0}^{s}\sum_{j=0}^{s} P_{ij}^{A}\log_2 P_{ij}^{A} + \sum_{i=s+1}^{L-1}\sum_{j=s+1}^{L-1} P_{ij}^{B}\log_2 P_{ij}^{B}\right]$$

The larger the local entropy, the more balanced will be the ratio between the object and background in the binary image. The gray level *s* corresponding to the maximum value of $H_T(s)$ represents the optimal threshold value at recognition of objects from the threshold.

The exemplary results of the presented algorithms applied to the chosen eye fundus images representing three classes of cases, are illustrated in Fig. 4 [12]. Left column represents the original images and the right one – the segmented vessel tree structures. The images in the first two rows correspond to the healthy cases (class 1), the second two – to the first two stages of the hypertension (class 2) and the last two – to the advanced hypertension (class 3). We may observe important variations of the structures of different images.

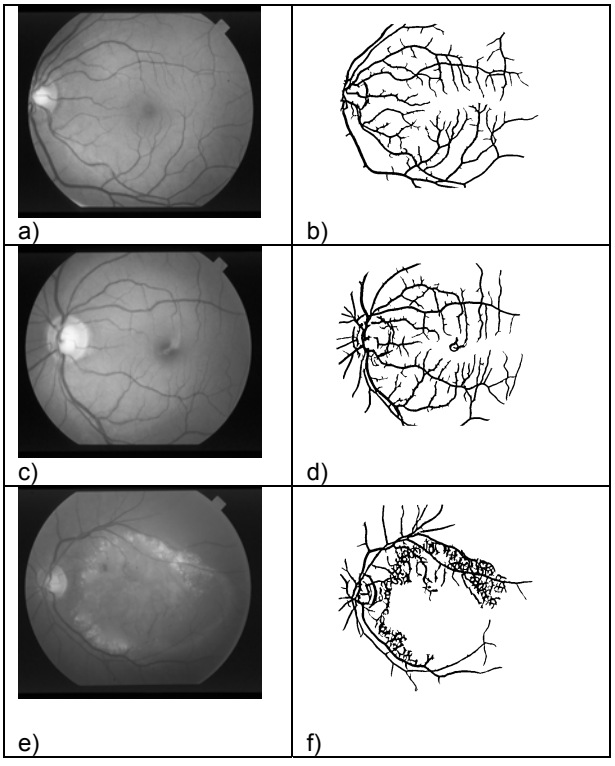

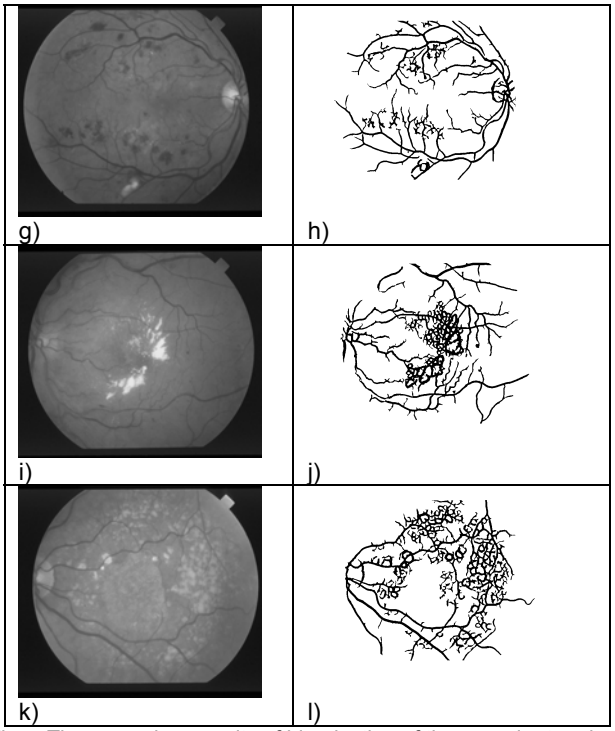

Fig. 4 The exemplary results of binarization of the vascular tree in eye fundus

We are interested in the differences of numerical characterization of vessel tree structures corresponding to different stages of development of the hypertension. We associate them with the fractal measure of complexity, applying the box-counting dimension.

Box-counting dimension evaluation for retinal images

In our experiments we have examined 125 images of eye fundus taken from the web free library [12, 13]. All of them have been divided by the medical experts into three classes:

- 43 images representing healthy stage (class 1)
- 38 images of the first two stages of the hypertension (class 2)
- 44 images of advanced hypertension (class 3).

Each image was processed, leading to the extraction of vessel tree structure, as presented in the right column of Fig. 4. In the final step the box-counting fractal dimension was computed using Matlab environment [4]. The detailed analysis of these results show, that different classes are characterized by various slopes of the N(s) curve (different measures of box-counting dimension). After analyzing all 125 images we were able to find the mean and standard deviation of box-counting dimension for the considered three classes of images. Table 2 depicts their values corresponding to full set of the considered images. More advanced stages of illness are associated with higher mean values. Observe that in all considered cases the standard deviation of results is relatively low.

Table 2 The mean values and std of box-counting dimension of the set of vascular trees for three classes of patients

Box-counting dimension	Class 1	Class 2	Class 3
Mean	1,4417	1,5109	1,6076
Std	0,0307	0,0298	0,0372

Fig. 5 presents the graphical distribution of the values of box-counting dimension obtained in the experiments. The horizontal axis corresponds to the set of patients (changing

from 1 to 44) and vertical one to the actual value of box-counting dimension corresponding to each case.

It is evident that box-counting dimension values are grouped in three clusters corresponding to the classes. The cluster corresponding to the healthy class is very well separated from the group of advanced stage of illness (class 3), while the class 2 cases occupy the intermediate position, slightly interlacing with both groups.

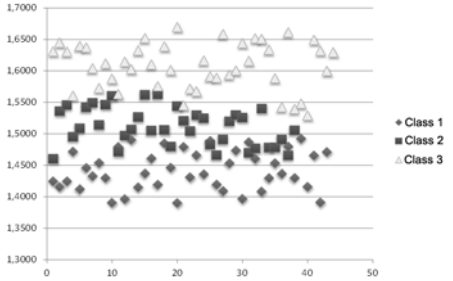

Fig. 5 The graphical visualization of the values of box-counting dimension for all investigated patients

Our results show an increase of fractal dimension with advanced disease, contrary to some other works [11], where the negative correlation was observed. This difference is due to the petechiae appearing in the eye fundus at advanced stages of hypertension, visible in images of Fig. 4. as a result we observe the increase of the total area of the vascular tree and also of fractal dimension.

Classification

Let us represent each of these three groups of data by their mean value. For the actual case we calculate the distance between the value of its box-counting dimension and the mean of each group. The minimal distance determines the membership to the particular class. The statistical results concerning all cases in the form of the confusion matrix are given in Table 2. The diagonal elements of this matrix represent the number of well recognized cases. The non-zero value of the *ij*th off-diagonal element indicates what number of *i*th class was recognized as the *j*th one.

Table 2 The confusion matrix of classification of the degree of development of hypertension on the basis of box-counting dimension

	Class 1	Class 2	Class 3
Class 1	38	5	0
Class 2	5	32	1
Class 3	0	2	42

We can observe that none of the healthy cases was misclassified with the advanced stage of illness. The only errors appear at recognition of the neighboring classes. The average percentage error of all cases representing the considered three classes recognition was equal 10.4%.

Table 3 The confusion matrix of the classification of the healthy versus non-healthy on the basis of box-counting dimension

	Healthy	Non-healthy
Healthy	40	3
Non-healthy	5	76

The other interesting application of the proposed method of vessel tree classification is the recognition of only two classes of cases: healthy and non-healthy, without recognition of the degree of development of hypertension. This may be treated as the pre-selection of the changes in the eye fundus. The statistical results concerning this type of classification using box-counting dimension are presented in Table 3.

The recognition of healthy patients is done now with the accuracy higher than 93%. In the case of non-healthy individuals the recognition rate is also almost 93% and sensitivity 93.8%. The average percentage error of recognition of both classes was equal 6.4%.

This relatively small value confirms high diagnostic value represented by a very simple measure of the box-counting dimension in application to the recognition of changes in the vessel structure of the eye fundus.

Conclusions

The paper has presented the application of the box-counting fractal dimension to distinguish among different forms of vessel structures of the eye fundus, associated with the advancement of hypertension. It was proved that this particular fractal dimension measure may be fast, one-dimensional discriminative feature for the pre-selection of the eye fundus images changes, useful in recognition of healthy and non-healthy cases.

The results of numerical experiments performed on 125 cases have shown that application of this one-dimensional description of the eye fundus images results in a quick and non complex method allowing to preselect the healthy from non-healthy cases.

REFERENCES

1. Szczeklik, M. Tendera, Kardiologia, Wydawnictwo Medycyna Praktyczna, Kraków 2010.
2. Sukumaran S., Punithavalli M., Retina recognition based on fractal dimension, *Intern. J. of Computer Science and Network Security*, vol. 9, 2009, pp. 66-70, 2009.
3. Schroeder M., Fractals, Chaos, Power Laws, 6 Ed. New York: W.H. Freeman and Company, 2006.
4. Matlab user manual, MathWorks, 2007.
5. Chanwimaluang T., Fan G., Fransen S. R., Hybrid retinal image registration, *IEEE Trans. Information Technology in Biomedicine*, vol. 10, 2006, pp. 129-142.
6. Chaudhuri S., Chaterjee S., Katz N., Nelson M., Goldbaum M., Detection of blood vessels in retinal images using 2-dimensional matched filters, *IEEE Trans. Med. Imag.*, vol. 8, 1989, pp. 263-269.
7. Hoover A. Kouznetsova V.,Goldbaum M., locating blood vessels in retinal images by piece-wise threshold probing of a matched filter response, IEEE Trans Medical Imaging, vol. 19, 2000, pp. 203-210
8. Pal N. R., Pal S. K., Entropic thresholding, *Signal Processing*, vol. 16, 1989, No 1, pp. 97-108.
9. Soille P., Morphological Image Analysis, Principles and Applications. Springer, Berlin; 2003.
10. Wagner T., Texture analysis (in Jahne, B., Haussecker,H. and Geisser P.,Eds., Handbook of Computer Vision and Application). Academic Press, pp. 275-309, 1999.
11. Wang J.J., Liew G, Cheung N, Zhang Y.P., Hsu W., Lee M.L., Mitchell P, Tikellis G, Taylor B, Wong T.Y., The retinal vasculature as a fractal: methodology, reliability, and relationship to blood pressure, vol. 115, 2008, pp. 1951-6
12. http://www.parl.clemson.edu/stare/probing/.
13. http://www.isi.uu.nl/Research/Databases/DRIVE/

***Authors**: dr inż. Michał Kruk, dr Bartosz Świderski, University of Life Sciences, Email: Krukmi1@poczta.wp.pl, prof. dr hab. inż. Stanisław Osowski, Warsaw Unversity of Technology and Military University of Technology, E-mail:* sto@iem.pw.edu.pl